A Dynamic Model for Dynamo Simulations in a Rotating Spherical Shell

Hiroaki Matsui (1,2) and Bruce A. Buffett (1)

(1.Dept. of Earth and Planetary science, Univ. California Berkeley 2. Dept. of Geophysical Sciences, the University of Chicago)

Introduction

Flow and magnetic fields in the outer core have a vast range of length scale from the size of the outer core to the thickness of the boundary layers. Numerical simulations cannot include the full range of scales, so sub-grid scale (SGS) models are required to account for the effexts of the unresolved fields on the large scale fields in geodynamo simulations. We previously performed a large-eddy simulation (LES) of a dynamo in a rotating plane layer model using the dynamic scale-similarity SGS model, and the LES using 24^3 grid represented a similar behavior of the flow and magnetic field to them obtained by 96^3 grid without the SGS model. In the present study, we implement this dynamic similarity model in a dynamo simulation in a rotating spherical shell.

We include terms for the SGS momentum and heat flux, the SGS Lorentz force, and the SGS magnetic induction. We also correct the commutation error caused by interchanging the order of the spatial differentiations and filtering operation. The amplitudes of the SGS term and commutation error correction are adjusted using model coefficients, which are evaluated automatically with a dynamic scheme, based on the Germano identity.

In the present study, we evaluate the model coefficient by the two approaches. One is that the coefficients are evaluated as a function of the radius r (so-called 1d-coefficient case), and another case is that the coefficients are evaluated as functions of the radius r and colatitude θ (2d-coefficient case).

Model of simulations

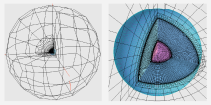

Figure 2: Finite element mesh for the rotating spherical shell model. Whole domain is displayed in the left, and closer view for the core is shown in the right. The domain for the outer core and inner core is plotted by blue and purple mesh, respectively. The cubed sphere is chosen for the grid pattern on each sphere, and non-equidistance grid is set in the radial direction. Coarser grid is also applied for external of the core and near center.

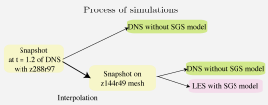

Table 1: Resolutions of the domain

Mesh	z288r97 (Resolved)	z144r49
Total num. of node	5.2×10^8	6.4×10^5
$\Delta\phi$ at equator (Deg.)	1.25	2.5
Num. of layer for fluid (r-direction)	96	48

- Inner core ($0 < r < r_i$): electrically conducted
- Outer core ($r_i < r < r_o$): conductive fluid
- External of the core ($r_o < r < r_m$): Insulator

Dimensionless numbers

$$Pr = \frac{\nu}{\kappa_\nu} = 1.0$$
$$E = \frac{\nu}{\Omega_0 L^2} = 5.0 \times 10^{-5}$$
$$Ra = \frac{\alpha g_0 \Delta T L}{\Omega_0 \nu} = 8.0 \times 10^2$$
$$Pm = \frac{\nu \Omega}{\eta} = 0.5$$

Boundary conditions

$$u_i = 0 \text{ at } r = r_i, r_o$$
$$T = 1 \text{ at } r = r_i$$
$$T = 0 \text{ at } r = r_o$$
$$A_i = 0 \text{ at } r = r_m$$

Sub-Grid Scale (SGS) Modeling

Grid filtering under numerical simulations

In numerical simulations, we can only treat resolved fields on simulation grids.

$$\bar{T}(\boldsymbol{x}) = \int T(\boldsymbol{x}') G^{\Delta}(\boldsymbol{x}-\boldsymbol{x}') dx' dy' dz'$$
$$G^{\Delta}(\boldsymbol{x}-\boldsymbol{x}') : \text{Filter function due to discretization}$$

Example: Thermal equation

$$\frac{\partial T}{\partial t} = -\frac{\partial}{\partial x_i}(u_i T) + Pr^{-1}\frac{\partial^2 T}{\partial x_i \partial x_i}$$

Thermal equation after filtering operation

$$\frac{\partial \bar{T}}{\partial t} = -\widetilde{\frac{\partial}{\partial x_i}(u_i T)} + Pr^{-1}\widetilde{\frac{\partial^2 T}{\partial x_i \partial x_i}}$$

$\downarrow$ Express equation in terms of filterd quantities

$$\frac{\partial \bar{T}}{\partial t} = -\frac{\partial}{\partial x_i}\left(\bar{u}_i \bar{T}\right) + Pr^{-1}\frac{\partial^2 \bar{T}}{\partial x_i \partial x_i} - \frac{\partial I_i}{\partial x_i} - \mathcal{D}_T^I(u_i T) + Pr^{-1}\mathcal{D}_{ii}^T(T)$$

Two type of additional terms to be modeled

1. Sub-grid scale (SGS) term: Heat flux
   Due to neglected correlations between u_i and T.
   $$I_i = \widetilde{u_i T} - \bar{u}_i \bar{T}$$
2. Correction for commutation error.
   Due to interchanging the order of filtering and spatial differentiations
   $$\mathcal{D}_T^I(u_i T) = \widetilde{\frac{\partial}{\partial x_i}(u_i T)} - \frac{\partial}{\partial x_i}\left(\bar{u}_i \bar{T} + I_i\right)$$

Basic equations for MHD simulation including SGS model

$$\frac{\partial \bar{u}_i}{\partial t} = -\frac{\partial \bar{\xi}_i}{\partial x_i} - \frac{\partial}{\partial x_j}(\bar{u}_j \bar{u}_i) + \frac{\partial^2 \bar{u}_i}{\partial x_j \partial x_j} - 2E\epsilon_{ijk}\Omega_j \bar{u}_k + Ra\bar{T}\hat{z}$$
$$+ Pm^{-1}E^{-1}\frac{\partial}{\partial x_j}\left(\bar{B}_i \bar{B}_j\right) - \frac{\partial}{\partial x_j}\bar{\tau}_{ij} + Pm^{-1}E^{-1}\frac{\partial}{\partial x_j}M_{ij}$$
$$-\mathcal{D}_{ji}^{\tau}(u_i u_j) + Pm^{-1}E^{-1}\mathcal{D}_j^M(B_i B_j) - \mathcal{D}_{ji}^{\alpha}(\chi) + \mathcal{D}_{ji}^{\mu}(u_i)$$
$$\frac{\partial \bar{T}}{\partial t} = -\frac{\partial}{\partial x_i}\left(\bar{u}_i \bar{T}\right) + Pr^{-1}\frac{\partial^2 \bar{T}}{\partial x_i \partial x_i} - \frac{\partial I_i}{\partial x_i} - \mathcal{D}_T^I(u_i T) + Pr^{-1}\mathcal{D}_{ii}^T(T)$$
$$\frac{\partial \bar{A}_i}{\partial t} = -\frac{\partial \bar{\phi}}{\partial x_i} + Pm^{-1}\frac{\partial^2 \bar{A}_i}{\partial x_j \partial x_j} + \epsilon_{ijk}\bar{u}_j \bar{B}_k + a_i - \mathcal{D}_i^B(\varphi) + Pm^{-1}\mathcal{D}_{ji}^B(A_i)$$
$$\left(\frac{\partial \bar{u}_i}{\partial x_i} + \mathcal{D}_i^{\tau}(u_i)\right) = \left(\frac{\partial \bar{A}_i}{\partial x_i} + \mathcal{D}_i^B(A_i)\right) = 0$$
$$\bar{B}_i = \epsilon_{ijk}\left(\frac{\partial \bar{A}_k}{\partial x_j} + \mathcal{D}_j^B(A_k)\right)$$
$$\bar{u}_i, \bar{T}, \bar{A}_i, \bar{B}_i, \bar{\chi}, \bar{\varphi}: \text{Filtered field}$$

SGS terms should be modeled for a geodynamo simulation

$$I_i = \widetilde{u_i T} - \bar{u}_i \bar{T} \quad : \text{SGS heat flux}$$
$$T_{ij} = \widetilde{u_i u_j} - \bar{u}_i \bar{u}_j \quad : \text{SGS momentum flux}$$
$$M_{ij} = \widetilde{B_i B_j} - \bar{B}_i \bar{B}_j \quad : \text{SGS Maxwell tensor}$$
$$a_i = \epsilon_{ijk}\left(\widetilde{u_j B_k} - \bar{u}_j \bar{B}_k\right) \quad : \text{SGS induction}$$

Nonlinear gradient model with dynamic scheme

The nonlinear gradient model is a version of the similarity model. We begin with discussion of the similarity model to introduce the dynamic version of the nonlinear gradient model.

Similarity model

Assumption:

- **Effects of sub-grid scale components are similar to those of resolved small scale**
- **Apply a second filter to evaluate the SGS terms using the smallest scale components of the resolved fields**

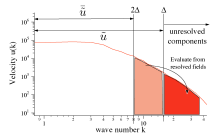

The SGS heat flux I_i is approximated by

$$I_i = \widetilde{u_i T} - \bar{u}_i \bar{T} \approx C^{sim}\left(\widetilde{\bar{u}_i \bar{T}} - \bar{\bar{u}}_i \bar{\bar{T}}\right)$$

where C^{sim} is a model constant. The second filter is applied to the resolved field (e.g. $\bar{T}$)

$$\bar{\bar{T}}(\boldsymbol{x}) = \int \bar{T}(\boldsymbol{x}') G^{2\Delta}(\boldsymbol{x}-\boldsymbol{x}') dx' dy' dz'$$
$$G^{2\Delta}(\boldsymbol{x}-\boldsymbol{x}') : \text{2nd filter function}$$

Nonlinear gradient model

The SGS terms are estimated using the Taylor expansion of the fields around the point of interest. To obtain the present model, we assume a symmetric filter with 0th and 1st moments equal to be 1 and 0, respectively. Under this assumption, the SGS terms are described by the product of gradients of the fields and a each direction of 2nd moment of the filter $\eta_k^{2\Delta}$ that depends on the width of the spa:ial filter.

$$I_i^{\Delta} \approx C^{sim}\left(\widetilde{\bar{u}_i \bar{T}} - \bar{\bar{u}}_i \bar{\bar{T}}\right) = C^{sim}\sum_k \eta_k^{2\Delta}\frac{\partial \bar{u}_i}{\partial x_k}\frac{\partial \bar{T}}{\partial x_k}$$
$$\eta_k^{2\Delta} = \int (x'_k - x_k)^2 G^{2\Delta}(\boldsymbol{x}'-\boldsymbol{x}) dx' dy' dz'$$

Advantage: Explicit filtering operation is not required for the nonlinear gradient model.

Commutation error correction

For an non-uniform grid (see Figure 2, for example) filter width should be proportional to the grid size to preserved the resolution. Under this condition, n-th moment of the filter varies with position. Considering the Taylor expansion and assumptions for the 0th and 1st moments of the filter for the nonlinear gradient model, the commutation error $\mathcal{D}(f)$ can be described approximately in terms of the 2nd order moment $\eta_i^{2\alpha}$

$$\mathcal{D}_i^I(f) \approx -\frac{1}{2}\sum_k \frac{\partial \eta_k^{2\Delta}}{\partial x_i}\frac{\partial^2 f}{\partial x_i \partial x_k} \approx -C^{dif} I \frac{1}{2}\sum_k \frac{\partial \eta_k^{2\Delta}}{\partial x_i}\frac{\partial^2 f}{\partial x_i \partial x_k}.$$

How do we evaluate the model coefficient C^{sim}?

A dynamic version of the nonlinear gradient model is developed using Germano's identity (1991)

$$\mathcal{L}_{Ii} = \widetilde{\bar{u}_i \bar{T}} - \bar{\bar{u}}_i \bar{\bar{T}} - I_i^{2\Delta} - I_i^{\Delta} \qquad (*)$$

where $I_i^{2\Delta}$ is also modeled by the nonlinear gradient model as

$$I_i^{2\Delta} = \widetilde{\bar{u}_i \bar{T}} - \bar{\bar{u}}_i \bar{\bar{T}}$$

and

$$I_i^{\Delta} = \widetilde{u_i T} - \bar{u}_i \bar{T}$$

The nonlinear gradient model can be used to approximate both $I_i^{2\Delta}$ and I_i^{Δ} assuming that the model coefficient is the same. Using the nonlinear gradient model for $I_i^{2\Delta}$ and I_i^{Δ} in the Germano identity (*) yields an equation where C^{sim} is the only unknown. Germano identity is solved for C^{sim} by using the least square method. In the present study, we compare the evaluation of the model coefficients C^{sim} over the zonal direction (as unctions of radius and colatitude) and the evaluation over each sphere (as a function of radius).

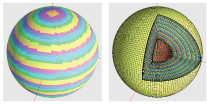

Figure 1: Grouping for evaluation of the dynamic model. For the 2d-coefficient model, elements are divided into groups xith respect to the colatitude and radius of the center of the element (left). For the 1d-coefficient model, elements are divided into groups by the radius of the center of the elements (right).

Results

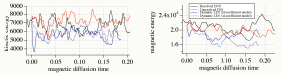

Figure 3: Time evolution of the spatially averaged kinetic (left) and magnetic energies (right).

Table 2: Average kinetic and magnetic energies between $t = 0.1$ and $t = 0.18$

Mesh	z288r97		z144r49	
	DNS	DNS	2d-coef.	1d-coef.
Kinetic energy	6.48×10^3 (100%)	7.72×10^3 (119%)	5.18×10^3 (88%)	5.91×10^3 (91%)
Magnetic energy	2.01×10^3 (100%)	2.07×10^3 (103%)	1.84×10^3 (92%)	1.62×10^3 (81%)

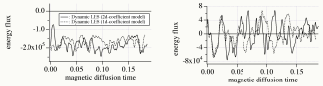

Figure 4: Time evolution of the spatially averaged work of SGS Lorentz force (left) and energy flux of SGS induction term (right).

Table 3: Average energy flux of resolved terms between $t = 0.1$ and $t = 0.18$.

Mesh	z288r97	z144r49		
	DNS	DNS	2d-coef.	1d-coef.
Buoyancy flux	1.98×10^4 (100%)	2.18×10^4 (110%)	1.48×10^4 (75%)	1.48×10^4 (75%)
Work of Lorentz force	-9.31×10^3 (100%)	-8.78×10^3 (94%)	-6.71×10^3 (72%)	-6.12×10^3 (66%)

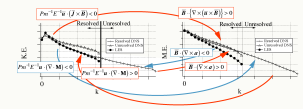

Figure 5: Energy transfer between kinetic and magnetic energies in the Large-eddy dynamo simulation. Work of Lorentz force indicates Energy flux from resolved kinetic energy to magnetic energy, and work of SGS Lorentz force and energy flux of SGS induction term show energy transfer between resolved and unresolved field.

Table 4: Average energy flux of SGS terms between $t = 0.1$ and $t = 0.18$. These results are compared values estimated directly from the fully resolved DNS with z288r97 mesh.

	D. estimation	modeled	
		2d-coef.	1d-coef.
SGS Lorentz force	-1.45×10^6 (100%)	-1.85×10^5 (13%)	-1.67×10^5 (11%)
Reynolds Stress	1.64×10^5 (100%)	-8.38×10^4 (-51%)	-8.34×10^4 (-51%)
SGS induction	2.06×10^6 (100%)	3.02×10^5 (0.15%)	1.94×10^5 (0.094%)

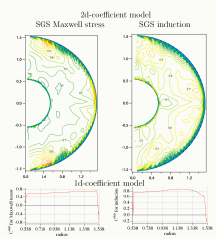

Figure 6: Model coefficients C^{sim} for SGS Maxwell tensor (left panels) and for SGS induction terms (right panels) averaged between $0.1 < t < 0.18$. Results by the 2d-coefficient model are plotted by the contour plot in the upper panels (contour interval is 0.05), and results by the 1d-coefficient model are plotted by line in the lower.

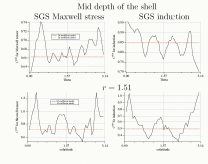

Figure 7: Model coefficients C^{sim} for SGS Maxwell tensor (left panels) and for SGS induction terms (right panels) averaged between $0.1 < t < 0.18$ as a function of colatitude θ. Results by the 2d-coefficient model are plotted by black, and results by the 1d-coefficient model are plotted by red.

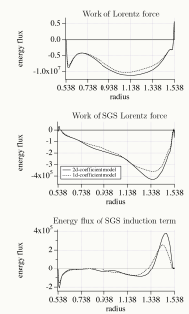

Figure 8: Work of (resolved) Lorentz force (top), SGS Lorentz force (middle), and energy flux of SGS induction term (bottom) integrated over sphere as a function of radius r. Results by the 2d-coefficient model are plotted by solid line, and results by the 1d-coefficient model are plotted by dotted line.

Conclusions

- Use of 2d model coefficients decrease the discrepancy between the time averaged magnetic energies in the dynamic LES and DNS. However, the discrepancy in the kinetic energy is not substantially improved by using 2d coefficients, relative to the use of 1d coefficients model (see Fig. 3 and Table 2).
- The buoyancy flux in the LES is approximately 75% of the buoyancy flux of the DNS at the same resolution. The difference is probably due to the role of the SGS heat flux in the LES. The other SGS terms are much smaller than those evaluated directly from the resolved DNS. (see Table 3)
- Work of the SGS Lorentz force is primary negative, indicating that the resolved kinetic energy is transferred to unresolved magnetic energy. On the other hand, energy flux of the SGS induction term changes its sign frequently, and its time average becomes small positive value. This result suggests that direction of the energy transfer between resolved magnetic field and unresolved convection often changes. (see Table 4)
- Model coefficients C^{sim} for the SGS induction term and SGS Maxwell tensor become large on the tangential cylinder and around equator (see Figure 6). The variation in the θ direction is small in the mid-depth (18% and 93% for SGS Maxwell tensor and SGS induction). Much larger variations in theta are observed near the outer boundary (100% and 150% for SGS Maxwell tensor and SGS induction at $r = 1.5$). The model coefficients obtained in the 1d and 2d model are roughly the same outside the tangent cylinder. (see Figure 7)
- The model coefficients has large variation in θ direction near the outer boundary. And, energy flux of SGS induction term and work of the SGS Lorentz force has a maximum amplitude at $r = 1.47$ and $r = 1.34$, respectively (see 8. These variations are not represented by the 1d coefficients, so that the largest differences between the two dynamic LES models occur in the SGS induction term near the outer boundary.
- Applying the evaluation of the C^{sim} over the zonal direction is slightly improved in the magnetic energy averaging over sphere and times. However, work of SGS Lorentz force and energy flux of the SGS induction term is significantly smaller than the work computed from the resolved calculations (see Table 4). The 2d-coefficient model can improve the present dynamic similarity model near the outer boundary, but we can also apply 1d-coefficient model in the other part of the shell. Further testing of the large scale fields (such as the dipole component of the magnetic field) is required to assess the validity of the SGS models. We also need to explore the use of different resolutions and parameter schemes.